Study of interaction of C^+ ion beam with a Si pitch grating on a macro-scale level

Andreas Mutzke[1], Ivan Bizyukov[2], Hagen Langhuth[3], Matej Mayer[3], Karl Krieger[3], Ralf Schneider[4]

[1] *Max-Planck-Institut für Plasmaphysik, EURATOM Association, Wendelsteinstr. 1, 17491 Greifswald, Germany*
[2] *Karazin Kharkiv National University, Faculty of Physics and Technologies, 31 Kurchatov Ave., Kharkiv 61108, Ukraine*
[3] *Max-Planck-Institut für Plasmaphysik, EURATOM Association, Boltzmannstr. 2, 85748 Garching, Germany*
[4] *Institute of Physics, Ernst-Moritz-Arndt University, Felix-Hausdorff-Str. 6, 17489 Greifswald, Germany*

Abstract

A Si pitch grating has been exposed to a 6 keV C^+ ion beam at normal angle of incidence and at an angle of 42° parallel to the structure. Sputtering of the grating has been observed experimentally by Rutherford backscattering, the areal density of implanted C ions into the Si structure has been measured by nuclear reaction analysis. The bombardment has been simulated by the SDTrimSP-2D code at normal angle of incidence, as well as at angles of 42° parallel and perpendicular to the structure. The numerical simulations show reasonable agreement with experimental results. Significant differences in Si sputtering and implantation of C ions parallel and perpendicular to the structure indicate an anisotropy effect, which could not be observed in the 1D case.

Keywords: SDTrimSP-2D, sputtering, reflection, roughness, ion-surface interactions.

PACs numbers: [reserved for the case if needed]

1. Introduction

Sputtering is an effect, which can be observed when energetic ions interact with a surface creating subsequent removal of target atoms [1]. Understanding of sputtering by gaseous ions is based on a large number of projectile-target combinations, which have been studied experimentally and by simulations; generally a good agreement has been observed in most cases [2]. In contrast, ions of non-volatile species do not leave the surface after penetration and deceleration; this process is called implantation. In this case implantation will produce mixed surfaces consisting of target atoms and projectiles and, in some cases, a deposition layer on top of the target surface consisting of decelerated projectile atoms [3]. The simulation of the interaction of non-volatile ions with a surface is a rather complicated problem, because the surface composition changes dynamically with fluence due to implantation and sputtering.

Presently existing numerical models are able to simulate a 1D surface, where the concentration of implanted species varies with depth. For example, a good agreement between simulation and experiment has been observed in [4], where the implantation of C^+ ions in a tungsten surface has been investigated. The well-known TRIDYN code [5] has been used for simulation of erosion yields and depth profiles. It has been recently revised in order to provide a clear modular structure to allow also easier physics extensions by adding new modules. The revised version of the code has been named SDTrimSP [6].

A new SDTrimSP code version being capable to simulate bombardment of a surface varying in 2 dimensions has been titled as SDTrimSP-2D [7]. This version allows to define a surface with variation not only as function of depth but also in one lateral dimension and model its evolution. A number of studies have been performed to validate this SDTrimSP-2D code comparing the simulation results with experiments from irradiation of a periodical Si pitch grating structure with Ar^+ [8], [9] and C^+ [10] ions. In these experiments a Si diffraction lattice has been used as a target. While results of simulations for volatile Ar^+ ions, which do not become implanted, were experimentally validated on both micro- and macro-scale, up to now the macroscopic parameters of the interaction of a non-volatile species (here C^+ ions) with a Si pitch grating have not been investigated yet.

In this work, macroscopic parameters of irradiation of a Si pitch grating with C^+ ions have been measured. The total erosion of Si has been measured using Rutherford back-scattering (RBS), while the areal density of implanted C atoms has been measured using Nuclear Reaction Analysis (NRA); both measurements have been performed *in-situ* as a function of incident fluence. Experimental data were compared to results of simulations with the SDTrimSP-2D code, which was used previously in [10] to follow the evolution of the surface morphology. In this work, SDTrimSP-2D with the same input parameters as in [10] has been used to simulate total areal densities of elements, total sputter yields and reflection coefficient. Further simulations show anisotropy effects, which could be observed also experimentally at irradiation of a 2D surface: irradiation of the pitch grating at inclined angle of incidence both parallel and perpendicular to the grating structure leads indeed to different fluence dependent dynamics of sputter yield, reflection and implantation. These results complement our previous findings, in so far as the evolution of the surface morphology observed in [10] can now be correlated also to total sputter yields and areal density of implanted C atoms.

2. Experimental

The experiments were performed using the Dual-Beam Experiment facility at IPP Garching [11]. The Si pitch grating was exposed to a 6 keV C^+ ion beam, which has been generated by a Sputter ion beam system. The ion beam was mass-separated by a 30° bending magnet and focused on the surface of the grating with a 3 mm ion beam spot. The sample holder can be rotated, so the angle of incidence can be changed from 0 to 42°. The sample can be installed on the target holder in such a way that inclined bombardment can be performed parallel to the grating structure. The pitch grating and respective angles of incidence are shown in Figure 1. The bombardment was performed at room temperature of the surface.

The Si pitch grating sample has been taken from the same set of samples as the ones used in [8], [9] and [10]. Its period is 500 nm and the height is 200 nm, the deviation from these values is within 5-20 nm, as measured by scanning electron microscopy. The structure has been created on top of a Si wafer, covered with a Ta interlayer, which has been introduced for labeling purposes. The cross-section of the pitch grating is shown in Figure 2.

Sputtering of the pitch grating was observed by means of RBS at the Tandem accelerator at IPP Garching [12]. A 2.5 MeV ^{3}He beam at normal incidence was used. RBS analysis has been used to measure the Si areal density. The RBS detector was a solid-state detector with an energy resolution of 15 keV and a solid angle of about 1.58 msr at a scattering angle θ = 165°. The sample was oriented in such a way that the grating structure was parallel to the exit beam. At this geometry correlation effects, such as incidence through a valley and exit through a hilltop, do not play a role. The areal density of implanted C has been measured using the nuclear reaction $^{12}C(^{3}He, p_1)^{14}N$. The protons from the nuclear reaction were detected with a large solid angle detector at a reaction angle of 120°. The detector was covered with an absorber foil for the backscattered ^{3}He ions. A detailed description of sample arrangement and measurement procedures could be found in [11].

The experimental procedure was as follows: after a first NRA and RBS analysis of the virgin sample the surface was sputtered by bombardment with a 6 keV C^+ ion beam. After this sputtering step, the sample was analyzed again by the MeV ^{3}He beam followed by another sputtering step. In the DBE installation sputtering and subsequent surface analysis can be performed in the same setup without breaking the vacuum. The diameter of the MeV analyzing beam was 1 mm, while the diameter of the 6 keV C^+ ion beam was ≈3 mm [11].

Computer simulations of RBS and NRA spectra were performed using the code SIMNRA 6.50 [12]. RBS spectra of the grating structure are calculated by using a linear superposition of sub-spectra, as described in [13]. SIMNRA 6.50 allows usage of arbitrary layer thickness distribution functions supplied by an input file. Correlation effects, such as incidence through a valley and exit through a hilltop or multiple surface crossings, are neglected. This is a reasonable approximation for the sample orientation used in the experiments, as discussed before.

3. Computer simulations

The simulations have been performed by the SDTrimSP-2D code [7]. 6 keV C^+ ions have been launched towards the surface consisting of Si atoms, which is shaped in two dimensions (vertical and lateral) and extended in the third dimension. It can be run in static or dynamic mode (SD) on sequential or parallel systems (SP). SDTrimSP-2D uses a 2-D mesh to represent the surface morphology, the first dimension is the direction perpendicular to the macroscopic surface plane, and the second is in a direction parallel to that plane. This representation is sufficient to simulate the ion bombardment of surfaces with 2D micro-structure extended into the 3rd dimension. It shares the same physical model of ion-surface interactions with other codes of the TRIM family. However, the resolution of a second dimension requires a 2-D domain with separate cells.

The code follows the density changes in the target material due to projectile and recoil particles coming to rest after a complete slowing-down at the end of their trajectories. In SDTrimSP/TRIDYN, this is done by a 1-D relaxation of the cells. Each trajectory creates a mass flux in the cells it passes. These fluxes can act as sink or source terms for the particle densities. To ensure particle conservation within the numerical setup, which uses a 1D grid of cells in which each cell has a constant volume density according to the material, volume changes of the 1D cells (expansion or contraction perpendicular to the surface) are used to represent changes to the number of particles in a cell. In SDTrimSP-2D, this procedure has been extended to 2D, subject to the requirement that all volume changes applied are divergence free. This reflects particle conservation in the projectile-target system expressed by volume changes. For each cell, the resulting mass fluxes (representing the transfer of particles into or out of the cell) are taken to be anisotropic by introducing the anisotropy coefficient (K_{anis}) of the volume relaxation. This anisotropy coefficient defines the ratio of volume changes, representing mass fluxes towards to the surface and volume changes, representing mass fluxes in lateral directions. The transport to the surface is usually set greater than those in lateral directions, because resistance against swelling or shrinking towards the surface is smaller.

In the simulations presented here an anisotropy coefficient of 0.5 was used. This anisotropy coefficient was obtained by calibration against experiments in previous works [8], [10]. Thus, the cells at the surface exposed to incident ions can change in two directions. The volume of cells without sides bordering on the surface is kept fixed. The relaxation process is done in several iterations until the divergence of the mass fluxes (transfer of particles between cells) becomes zero and steady-state conditions without internal tension are obtained. From this steady-state, divergence-free solution the volume changes are applied. In addition, splitting and annihilation of cells was introduced in SDTrimSP-2D, according to a maximum and minimum number of atoms, to be able to represent creation of holes or strong deposition.

Since the surface is a periodic structure in the lateral direction, periodic boundary conditions in this direction are used.

4. Results and discussion

The pitch grating has been exposed at normal angle of incidence and at inclined angle of 42° parallel to the grating structure. The areal densities of Si and C have been measured and simulated by means of the SDTrimSP-2D code. Therefore, the obtained results represent macroscopic characteristics of the interaction of C ions with the Si pitch grating structure.

The comparisons of the experimental data and simulation are shown in Figure 3. Typically for this kind of experiments, the areal density of C atoms is growing due to implantation. The areal density of Si is decreased due to sputtering until the surface of the pitch grating is completely covered by a "layer" of implanted C atoms, which prevents further sputtering of Si atoms. For normal angle of incidence the simulation matches almost exactly the experimental result. As one can see in [10], on the nanometer-scale level tops and valleys of the pitch grating are covered by layer of implanted C. No significant redeposition of C and Si is observed on the vertical walls of the grating. Instead, the walls are the source for highest local sputtering yield. The thickness of the grating features decreases with the fluence because it appears to be the only location, where Si erosion occurs.

In the case of inclined bombardment, the simulated evolution of the Si areal density with bombardment fluence deviates from the experimental results. The erosion rate observed in the experiment is twice as high as that predicted by the model. This disagreement is typical for those angles of incidence, where erosion of the target is closely balanced by implantation of non-volatile ions. A similar effect has been observed at irradiation of W surface with 6 keV C^+ ions at an inclined angle in [14], where the strongest disagreement between the experiment and modeling has been observed at an angle of 35°. At the same time, the simulation still accurately matches the measured implantation rate of C ions. On a nano-scale level, implanted C atoms replace sputtered Si atoms in the way that the level of the valleys does not change relatively to the Ta layer (see Fig. 6 in Ref. [10]).

Experiment and simulation both include both systematic and statistical errors, which although small, in combination can explain the observed disagreement. The measured areal density of Si and C are accurate within about 5%, which is typical for RBS and NRA measurements. Although Si is difficult to be seen directly because it is on top of the Ta signal, the high-energy edge of the intermediate Ta layer is shifted by the Si layer on top, which is a very sensitive measure of the surface amount of Si. The error of the fluence measurement is expected to be smaller than 10% because experiment and simulation closely match for Si sputtering at normal incidence angle, as well as C implantation at normal and inclined incidence. Other factors related to experiment, which may contribute to the disagreement, are deviations of the actual surface profile from what has been used as input into the SDTrimSP-2D code and small contaminations of the pitch grating with carbon, which is observed as non-zero areal density of carbon detected by NRA prior to irradiation. On the modeling side, the surface binding energies, which enter the simulation, vary from pure carbon (its surface binding energy depends on crystalline structure) to Si-C mixture. These factors appear to be negligible at normal angle of incidence. However, their contribution becomes significant at an inclined bombardment and produces the noticeable deviation between simulation and experiment.

The fluence dependent evolution of the surface sputtering yields for C and Si, as well as that of the reflection coefficient is shown in Figure 4. The results have been obtained by simulations for the cases of normal angle of incidence and of bombardment at 42° incidence angle both oriented perpendicular and parallel to the 2D grating structure. The evolution of the macro-scale parameters of ion-surface interactions varies between normal incidence and incidence at inclined angles. Similar differences have also been observed in the 1D case. The 1D simulation obviously can not reproduce the different behavior of irradiation at the same inclined angle for different orientation of the incident ion beam relative to the pitch grating structure. The 2D simulation of the corresponding system clearly reproduces the anisotropy effect, which is determined by the geometry of the surface. Comparing the simulations for 1D and 2D surfaces, one can see well expected differences. 2D structure introduces as an additional element the appearance of roughness, resulting in an increase of the sputtering yield of Si and a reduction of the reflection coefficient of C^+ ions due to redeposition.

One can see in Figure 4 that sputter yield and reflection coefficient for normal incidence is typically lower than for an inclined angle of bombardment. This is the expected behavior for ion sputtering in this energy range. However, there are additional significant differences for inclined irradiation of laterally non-uniform surfaces depending on the orientation of the surface towards the incident ions: for the grating morphology discussed in this study, the bombardment parallel to the grating structure produces always higher sputtering and reflection of incident ions. This can be explained well by the fact that redeposition of reflected C ions and sputtered atoms is higher, when the ions enter the surface perpendicular to the structure. The details of local ion-surface interactions at the pitch grating surface are discussed in [10]. It has been shown that a surface with pronounced 2D morphology provides opportunities for sputtered and reflected atoms to be re-deposited again; such opportunity does not exist in case of 1D planar surface.

A local increase of the Si sputter yield for the case of perpendicular bombardment in the fluence range $(700\text{-}1200)\times10^{15}$ cm^{-2} is particularly interesting, because it breaks up the monotonically decreasing trend due to implantation of C ions and covering of the structure with a C layer. The dynamic evolution of the Si sputter yield shows a local maximum in this fluence range; such behavior cannot occur in the 1D case. The explanation for this anomaly is the local dynamics of ion-surface interactions on the nanometer-scale. As one can see in [10] (Fig. 9), the inclined bombardment tends to produce a layer on the side of the surface elevation shadowed from direct ion impact while the ion exposed side is eroded. The dynamics of the ion-surface interactions in this fluence range leads for certain exposure conditions to increased exposure and, consequently, sputtering of the Si surface instead of monotonic increase of implantation and growth of C layer. This opposite behavior depends purely on geometrical factors and manifests itself in corresponding changes of the dynamics of sputter yields and reflection at inclined bombardment perpendicular to the structure.

5. Conclusions

Si pitch gratings have been exposed to a 6 keV C^+ ion beam both at normal angle of incidence and at an angle of 42° parallel to the grating structure. The removal of Si atoms as a function of fluence has been measured by RBS, and at the same time, implantation of C ions has been measured by NRA *in-situ*. The obtained results have been compared to numerical simulations by the SDTrimSP-2D code. As previously shown for the case of volatile bombarding species, the comparison has confirmed that the SDTrimSP-2D code reproduces the macro-scale parameters of ion-surface interactions for a 2D structured surface, also for the case of non-volatile ions. Further simulations for macroscopic parameters have been performed for normal angle of incidence and inclined angles of incidence parallel and perpendicular to the investigated 2D surface structure. The simulations have revealed a strong influence of the surface morphology. This includes a strong anisotropy effect, with the sputtering at inclined angle of incidence varying between the cases of ion incidence parallel to the surface structure and perpendicular to the surface structure respectively. In addition one observes an increase of the Si sputter yield in a narrow fluence range. Both effects do not occur in a 1D system with planar surface. This investigation supplements our previous investigation [10], where the SDTrimSP-2D code has been used for simulation of morphology evolution of 2D structures. In this previous study experimental uncertainties in fluence measurement at the particular location had prevented a full quantitative validation of the code at that time.

References

1 R. Behrisch (ed). *Sputtering by Particle Bombardment. I. Physical Sputtering of Single-Element Solid*. ISBN 978-3-540-10521-3 (Berlin, Springer, 1979).

2 R. Behrisch, W. Eckstein (ed). *Sputtering by Particle Bombardment. Experiments and Computer Calculations from Threshold to MeV Energies*. ISBN 978-3-540-44500-5 (Berlin, Springer, 2007).

3 R. Behrisch (ed). *Sputtering by Particle Bombardment. II. Sputtering of Alloys and Compounds, Electron and Neutron Sputtering, Surface Topography*. ISBN ISBN 978-3-540-12593-8 (Berlin, Springer, 1983).

4 I. Bizyukov, K. Krieger, N. Azarenkov, and U. Toussaint. *Relevance of surface roughness to tungsten sputtering and carbon implantation*. J. Appl. Phys. vol.**100**, 113302, (2006).

5 W. Moeller, W. Eckstein, and J. P. Biersack. *TRIDYN - binary collision simulation of atomic collisions and dynamic composition changes in solids*. Comput. Phys. Commun. vol.**51**, pp. 355-368, (1988).

6 W. Eckstein, R. Dohmen, A. Mutzke, and R. Schneider. *SDTrimSP: A Monte-Carlo Code for Calculating Collision Phenomena in Randomized Targets*. IPP Report 12/3 (Garching, Max-Planck-Institute for Plasmaphysics, 2007).

7 A. Mutzke, R. Schneider. *SDTrimSP-2D: Simulation of Particles Bombarding on a Two Dimensional Target Version 1.0*. IPP Report 12/4 (Garching, Max-Planck-Institute for Plasmaphysics, 2009).

8 I. Bizyukov, A. Mutzke, R. Schneider, and J. Davis. *Evolution of the 2D surface structure of a silicon pitch grating under argon ion bombardment: Experiment and modeling*. Nucl. Instr. and Meth. vol.**B268**, pp. 2631-2638, (2010).

9 I. Bizyukov, A. Mutzke, M. Mayer, H. Langhuth, K. Krieger, R. Schneider. *Macroscopic parameters of the interaction of an* Ar^+ *ion beam with a Si pitch grating*. Nucl. Instr. and Meth. vol.**B 278**, pp. 4-7, (2012).

10 A. Mutzke, I. Bizyukov, R. Schneider, and J. Davis. *Nano-scale modification of 2D surface structures exposed to 6 keV carbon ions: Experiment and modeling*. Nucl. Instr. and Meth. vol.**B269**, pp. 582-589, (2011).

11 I. Bizyukov, K. Krieger. *Dual beam experiment for simultaneous irradiation of surfaces with ion species of gaseous and solid-state elements*. Rev. Sci. Instrum. vol.**77**, 043501, (2006).

12 M. Mayer. *SIMNRA User´s Guide.* Report IPP 9/113, Max-Planck-Institut für Plasmaphysik, Garching, Germany 1997.

13 H. Langhuth, M. Mayer, and S. Lindig. *Layer morphology analysis of sputter-eroded silicon gratings using Rutherford backscattering*. Nucl. Instr. And Meth. vol. **B269**, pp. 1811-1817 (2011).

14 W.Eckstein, J.Roth. *Sputtering of tungsten by carbon*. Nucl. Instr. and Meth. vol. **B53**, pp. 279-284 (1991).

Figure Captions

Figure 1. Directions of ion incidence relative to the pitch grating structure: (a) – normal angle of incidence, (b) – incidence at an angle of 42° parallel to the structure and (c) – incidence at an angle of 42° perpendicular to the structure.

Figure 2. The cross-section showing the structure of the Si pitch grating sample as obtained by scanning electron microscopy.

Figure 3. Comparison of the experimentally measured and numerically simulated fluence dependent variation of Si and C areal density. (a) – normal angle of incidence, (b) – incidence at an angle of 42° parallel to the structure.

Figure 4. Total sputter yield of Si (a); total self-sputter yield of C (b) and reflection coefficient (c) as a function of fluence as obtained by numerical simulation. Each graph compares data for the three angles of incidence: normal incidence and inclined angles of 42° parallel and perpendicular to the grating structure. Black lines show results of simulations for 2D surface, red lines correspond to 1D plane surface.

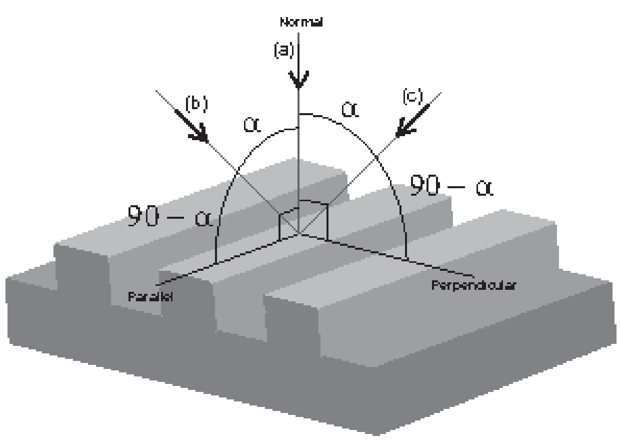

Fig 1

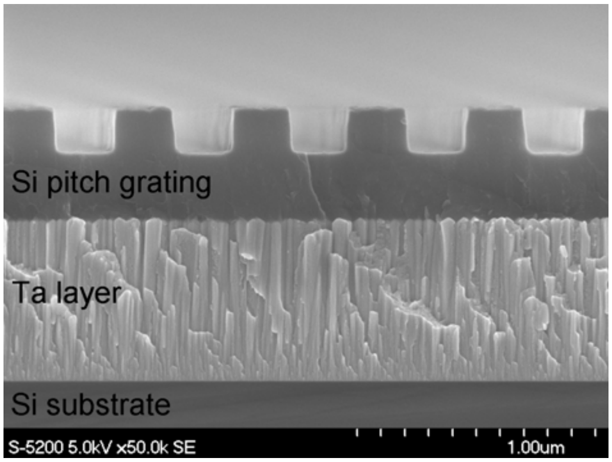
Si pitch grating
Ta layer
Si substrate
S-5200 5.0kV x50.0k SE
1.00um

Fig 2

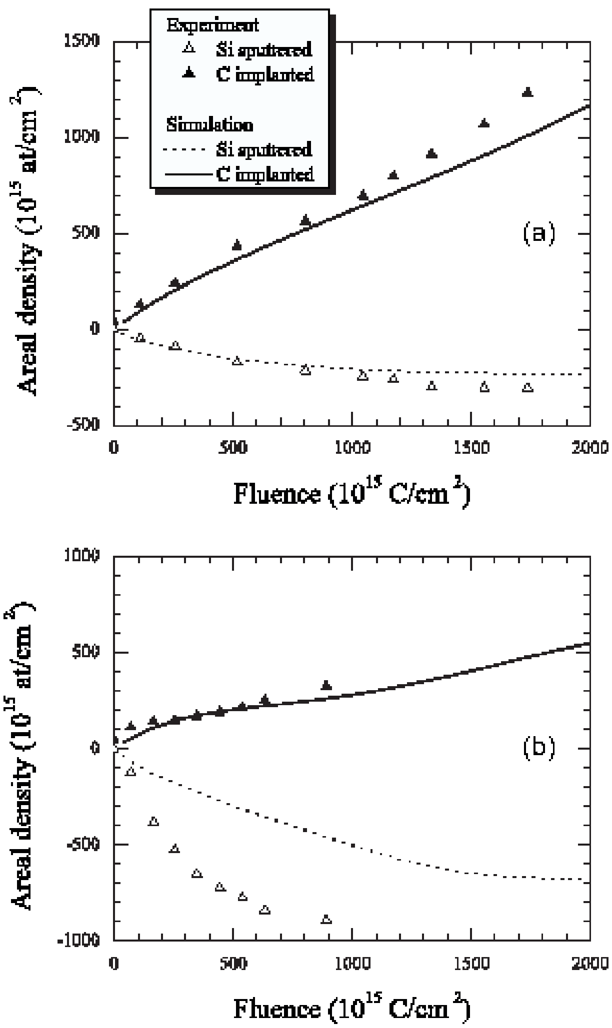
Experiment
Si sputtered
C implanted
Simulation
Si sputtered
C implanted
(a)
(b)
Areal density (10^15 at/cm^2)
Fluence (10^15 C/cm^2)

Fig 3

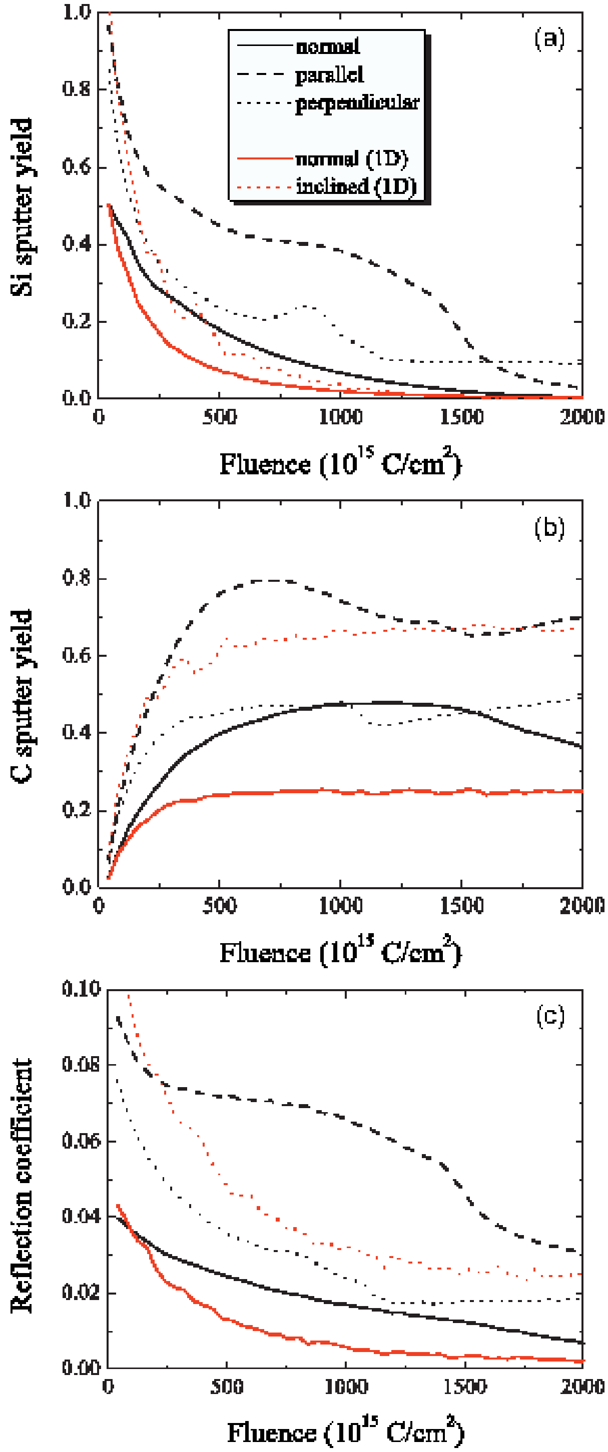
normal
parallel
perpendicular
normal (1D)
inclined (1D)
(a)
Si sputter yield
Fluence (10^{15} C/cm^2)
(b)
C sputter yield
Fluence (10^{15} C/cm^2)
(c)
Reflection coefficient
Fluence (10^{15} C/cm^2)

Fig 4